ReHILAE: is the Re-ionisation of Hydrogen-I the sole consequence of Lyman-alpha Emitters?

James Gold[1], Connor Donovan[1], Jack Bowden[1], James Carr[1], Joe Phillips[1] & David Sobral[1]*

[1] *Department of Physics, Lancaster University, Lancaster, LA1 4YB, UK*

ABSTRACT

The Epoch of Hydrogen Re-Ionisation (EoR) is an important stage in the evolution of the Universe, in which the neutral hydrogen in the Intergalactic Medium (IGM) becomes fully ionised. There are a number of ambiguities concerning the exact time period of the EoR, in addition to the exact nature of its causes. Previous methods describing this event use observations of Lyman Break Galaxies (LBGs), Lyman Alpha Emitters (LAEs - a subset of LGBs), and Active Galactic Nuclei (AGNs) as the predominant ionising sources of the EoR. With a few varying assumptions, galaxies appear to be the primary sources to consider. The UV-based framework currently used requires assumptions of the efficiency in converting between UV and Lyman-continuum (LyC) ionising photons (ξ_{ion}), and the fraction of LyC photons that actually escape their sources (f_{esc}). Direct measurements of these values using the UV-framework appear to produce values far below what are expected. Considering LAEs, which are a subset of the UV continuum, we can use varying data sources to comfortably approximate them as the sources with the highest production of ionising photons per UV luminosity. Therefore, by only considering LAEs, we can eliminate the need for determining ξ_{ion} entirely. Taking this approach, our own model for the fraction of ionised hydrogen in the Universe as a function of redshift ($Q_{H_{II}}$) was outlined. This model provided us with an approximate value of the LyC escape fraction as ~10%, which is a far more acceptable value than defined in previous studies. Comparing final results for $Q_{H_{II}}$ directly to our own improved UV-framework model, we determined that the re-ionisation of hydrogen is the sole consequence of LAEs.

Key words: Astrophysics, PHYS369, re-ionisation, Lyman-Alpha, LAEs, EoR.

1 INTRODUCTION

Understanding the evolution of the early Universe is an import topic in determining why the Universe is in its current form. Regarding the early Universe at a time of redshift z = 780 - 1150 (Landau et al. 2001), we can see that the recombination of hydrogen is observed to have completed across the IGM. This results in the IGM cooling to an acceptably low temperature for recombination to be energetically favourable (T ≈ 4100K, see Zeldovich et al. (1968)). This in turn then signals the era of the dark ages. Instead, moving to redshift z ≈ 10 (see Peebles (1993)), we see that sources capable of producing ionising photons above the Lyman Alpha limit, known as Lyman-continuum photons (LyC), start to form (Loeb & Barkana 2001), occurring when $\lambda \leq 912$ Å.

Previous work from Robertson et al. (2013) used a toy model simulation to analyse the volume change of ionised hydrogen as a fraction over changing redshift ($Q_{H_{II}}$). A key term in this expression is the the availability of ionising photons to the IGM ($\dot{n}_{ion}$): a paramount term, which is the main determinate when considering $Q_{H_{II}}$. Further terms of significance include the intrinsic escape fraction of ionising LyC photons (f_{esc}) used in $\dot{n}_{ion}$. This is used to determine the amount of ionising photons that actually escape from galaxies and is significant because a large percentage of photons produced in these galaxies are absorbed by the galaxies themselves (Gould & Schréder 1967). In addition to this, the size of the galaxy's dark matter halo also affects the escape fraction, where specifically the escape fraction is inversely proportional to the dark matter halo mass (Yajima et al. 2011; Wise et al. 2014; Wise & Cen 2009; Razoumov & Sommer-Larsen 2010). The varying f_{esc} of galaxies due to

* PHYS369 supervisor.

dark matter halos also effected how neutral hydrogen in the IGM was then re-ionised in bubbles around these sources until overlap occurred (see Thomas et al. (2009)), having fully ionised by redshift z ≈ 6 (Becker et al. 2001; Barkana 2002). In most studies the suggested fraction is at 10% - 20% (Bolton et al. 2011; Kimm & Cen 2014; Khaire et al. 2016) with the value being fixed with changing redshift. Results from Robertson et al. (2013) lead to the conclusion that re-ionisation could occur within the required range of 6 < z < 10. However, in the calculations they used, assumptions were made such that f_{esc} from sources were set to f_{esc} = 0.2 from Masami Ouchi (2009). Considering this, it doesn't seem possible to ionise the Universe by redshift z = 6 without higher values of f_{esc} due to the direct effect it has on the rate of re-ionisation. Conversely, Faisst (2016) introduces an expression of the escape fraction as a function of redshift which can be seen further discussed in 2.1. Although this expression leads to more promising results, the resultant re-ionisation time still needs work.

Concentrating on other terms in the equation for $\dot{n}_{ion}$, we can look at Faisst (2016), who made variations on the ionisation efficiency (ξ_{ion}) for different plots (see also Wilkins et al. (2016a)) using data obtained from Bouwens et al. (2016); Stanway et al. (2016); Wilkins et al. (2016b). The last part of $\dot{n}_{ion}$ used is the integrated UV luminosity density (ρ_{UV}) (see Mason et al. (2015)). Again, using the values from this paper, the correct re-ionisation time-frame is unlikely, but Faisst (2016) shows that it is still possible. Previous models discussed appear to focus on whether ionising sources could re-ionise the Universe. We intend to further research this idea and see if re-ionisation is possible using only LAEs as sources.

To do this we intend to use a modified version of the equation $\dot{n}_{ion}$ from Sobral & Matthee (2019), where ξ_{ion} and ρ_{UV} are replaced by the number of ionising photons (Q_{ion}). The reasoning for this is that not all ρ_{UV} photons are above the Lyman limit, therefore are not all LyC photons. This means that there is a range of photons of energy too low to ionise neutral hydrogen, in addition to a range of photons that can ionise which are above the limit of the UV spectrum in terms of energy. In light of this, calculations using ρ_{UV}, such as in Robertson et al. (2013) and Faisst (2016), appear to incorrectly estimate the total number of ionising photons being produced by ionising sources. When considering our own study, we are exclusively observing if Lyman Alpha Emitters (LAEs) can re-ionise the Universe alone in simulations. This means that all LyC photons will come from LAEs and all other sources will be ignored. In reality however, this would not be be the case due to the existence of other sources. Nonetheless, these other sources produce far less escaping photons and are therefore considered negligible (Ouchi et al. 2008).

Ionising sources include Lyman Break Galaxies (LBGs), LAEs; which are a subset of LBGs, and Active Galactic Nuclei (AGNs). LBGs are observed to have a significant drop in intensity at wavelengths shorter than the Lyman continuum ($\lambda \leq 912\text{Å}$) due to the hydrogen gas in the galaxy's ISM absorbing them. The emission of LyC photons in these galaxies allows them to ionise the IGM, and thus contribute to re-ionisation. It is worth noting however, that LBGs have a relatively low escape fraction of $f_{esc} \approx 6\%$ (Vanzella et al. 2010), whereas LAEs have a much higher

value (Mallery et al. 2012). We can therefore suggest that LAEs are a much larger contributor to re-ionisation. This is in part due to the fact LAEs have lower than typical masses ($10^8 M_\odot < m < 10^{10} M_\odot$ (Vallini et al. 2012)) which, as previously mentioned, results in their escape fraction being higher due to proportionally properties relating to galaxy masses. As a result of this, LAEs - a subset of LBGs - have been shown to have a much greater f_{esc} at high redshifts (Faisst 2016), and therefore are the main interest of this study. Additionally, it is worth considering AGNs, which are also producers of LyC photons due to the emissions from their high temperature accretion disks (Malkan 1983). They are thus also capable of contributing to the ionisation of the IGM. However Fontanot et al. (2012) suggests that given the current understanding of typical AGNs, and the relatively low f_{esc} of LBGs, we cannot conclude that AGNs are solely responsible for re-ionisation. Therefore their contribution is not accounted for in this study. To determine whether or not LAEs alone are capable of re-ionising the Universe in the agreed upon time frame we must first determine the average number of LyC photons produced per unit time by LAEs ($Q_{ion,Ly\alpha}$). Of this, the LyC production rate is directly proportional to Lyα luminosity ($L_{Ly\alpha}$). The rest-frame equivalent width (EW$_0$) of LAEs is used to determine the strength of the spectrum emitted light. This factor accounts for the effects of Doppler broadening due to the motions of sources that produce LyC photons (Chantry 1971). The data relating EW$_0$ and redshift can be found in Sobral et al. (2018). Combining this with the data relating the the rest-frame equivalent width (EW$_0$) and LyC escape fraction ($f_{esc}LyC$), and then taking the product of the Lyα luminosity and the LyC escape fraction, would then give us the number of LyC photons available for re-ionisation.

2   METHODOLOGY

2.1   The Robertson/Faisst Approach

To discover if LAEs are entirely responsible for re-ionisation, the differential equation given by Robertson et al. (2013) needs to be solved for $Q_{H_{II}}$ as a function of cosmic time:

$$\dot{Q}_{H_{II}} = \frac{\dot{n}_{ion}}{\langle n_H \rangle} - \frac{Q_{H_{II}}}{t_{rec}} \tag{1}$$

Where:

$$\dot{n}_{ion} = f_{esc}\xi_{ion}\rho_{UV} \tag{2}$$

$$n_H = 1.67 \times 10^{-7} \left(\frac{\Omega_b h^2}{0.02} \right) \left(\frac{X_p}{0.75} \right) \tag{3}$$

$$t_{rec} = \left[\alpha_\beta \langle n_H \rangle C_{H_{II}} \left(1 + \frac{Y_P}{X_P} \right) (1+z)^3 \right]^{-1} \tag{4}$$

$$\alpha_B = 2.6 \times 10^{-13} \left(\frac{T}{10^4} \right)^{-0.76} \tag{5}$$

$$C_{H_{II}} = \frac{\langle n_H^2 \rangle}{\langle n_H \rangle^2} \tag{6}$$

When concerning ourselves with the equations outlined

Table 1. A list of the constants and expressions used in equations 3 through to 6 taken from Robertson et al. (2013)[1], Planck Collaboration et al. (2016a)[2], and Liddle (1999)[3]

Parameter	Symbol	Value
Hydrogen Mass Fraction[3]	X_p	0.75
Helium Mass Fraction[3]	Y_p	0.25
Baryon Matter Density[2]	Ω_b	0.04
Cosmological Constant Density[2]	Ω_Λ	0.692
Parametrisation of Uncertainty in H_0 [2]	h	0.7
Hubble's Constant[2]	H_0	0.0692 Gyr^{-1}
IGM Temperature[1]	T	20000 K
Clumping Factor[1]	C	3

above, the constants defined in equations 3, 4, 5, and 6 are provided in table 1. With equation 2 however, there are numerous different approaches to defining the variables used. Specifically, we will look at the approaches taken by Faisst (2016) and Robertson et al. (2013). The latter uses data provided by Dunlop et al. (2013), in addition to data from models by Bruzual & Charlot (2003) to define $log(\xi_{ion})$ as 25.4 ± 0.1 Hz erg^{-1} On the other hand, Faisst (2016) uses data from Bouwens et al. (2015) to give ξ_{ion} as 25.4 Hz erg^{-1} and 25.6 Hz erg^{-1}. f_{esc} is given as:

$$f_{esc} = \frac{f_{esc,0}}{100}\left(\frac{1+z}{3}\right)^\alpha \tag{7}$$

where α is taken to be 1.17 ± 0.02 and $f_{esc,0} = 0.023 \pm 0.05$. Robertson et al. (2013) does not make use of this equation, and simply provides f_{esc} as 0.2 using data from Masami Ouchi (2009). In both cases, the techniques for determining ρ_{UV} are explicitly defined in their respective papers. With these parameters in mind, we will take our own approach to defining the variables in equation 2 and outline any changes we wish to make.

## 2.2 Perturbing Values from the Robertson/Faisst Approach

When determining ξ_{ion} in our own approach, we decided to utilise the following equation outlined in Matthee et al. (2016):

$$\log_{10}(\xi_{ion}) = 24.4 + \log_{10}(1+z) \tag{8}$$

This equation estimates results by taking observable values of the UV luminosity slopes of high redshift galaxies. Accompanying this, the redshift evolution for an average population of galaxies at z > 2.2 are inferred. This allowed us to perturb values of ξ_{ion} instead of keeping them constant. We approached defining ρ_{UV} by taking given data from Bouwens et al. (2015). Instead of using this data to define a single (or in the case of Faisst (2016), a couple) result(s), a cubic fit was taken, allowing us to vary it's value over a range of redshifts (Figure 1). The resultant expression used can be seen in equation 9.

$$\begin{aligned} log(\rho_{UV}) = &(0.0014^{+0.00090}_{-0.00090})z^3 + (-0.056^{+0.025}_{-0.025})z^2 \\ &+ (0.29^{+0.21}_{-0.21})z + (26^{+0.54}_{-0.54}) \end{aligned} \tag{9}$$

The results and comparisons of these fits can be seen in section 3.3. Once these comparisons are made, our method can be undertaken more comfortably.
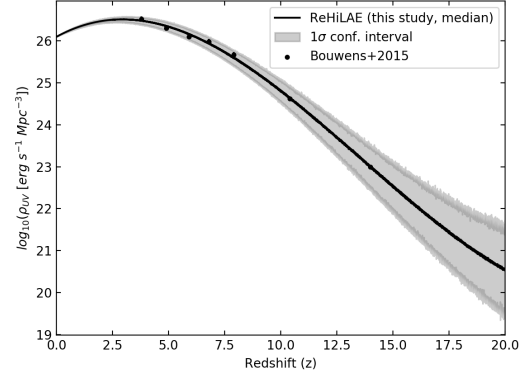
Figure 1. The median and 1σ spread of 1,000 iterations (see section 3.1) of ρ_{UV} (see equation 9) against redshift

2.3 The New Lyα Framework

As discussed in section 1, previous approaches to determining the fraction of ionised hydrogen utilise UV luminosity densities. This is despite the fact that not all UV photons are LyC photons. Thus, to more accurately determine the produced number of LyC, the equation in Sobral & Matthee (2019) was implemented.

$$Q_{ion,LyC}\left[s^{-1}\right] = \frac{L_{Ly\alpha}}{c_{H\alpha}(1-f_{esc,LyC})(0.042EW_0)} \tag{10}$$

where $c_{H\alpha} = 1.36 \times 10^{-12}$ erg. It can be seen that equation 10 gives the number of LyC photons produced per second, however what is required is the number of LyC photons produced per second per Mpc. Using data from (Sobral et al. 2018), $L_{Ly\alpha}$ can be replaced with $\rho_{Ly\alpha}$, yielding the following more functional equation:

$$Q_{ion,LyC}\left[s^{-1}\ Mpc^{-3}\right] = \frac{\rho_{Ly\alpha}}{c_{H\alpha}(1-f_{esc,LyC})(0.042EW_0)} \tag{11}$$
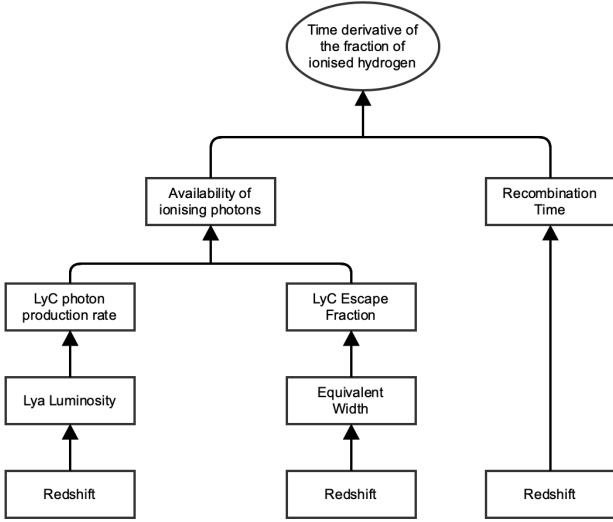
Dimensionally, this expression is equivalent to $\xi_{ion}\rho_{UV}$ but theoretically, it is a much better representation of the produced number of LyC photons. Subsequently, if multiplied by the average escape fraction of LyC photons of LAEs, the resultant equation would give an expression for the number of LyC photons produced per second per Mpc available for re-ionisation ($\dot{n}_{ion}$):

$$\dot{n}_{ion} = f_{esc,LyC}Q_{ion,LyC} \tag{12}$$

This led to the dependencies in our model as shown by figure 2.

2.4 Perturbing Values in the Lyα Framework

Taking into account the dependencies outlined in figure 2, and the equations 11 and 12, it is clear an expression describing the fraction of LyC photons from LAEs as a function of EW_0 is required. To begin determining this function, data from Sobral et al. (2018) was used to form a relation between EW_0 and redshift (see equation 13). With a usable relation between EW_0 and redshift now available, data was taken from Verhamme et al. (2016) to derive a simple linear expression relating the EW to the LyC escape fraction (see

Figure 2. Flowchart showing the dependencies in our new model using equation 12.

Figure 3. A plot showing the quadratic fit to the Lyα luminosity density (see equation 2.4). Any data taken from Sobral et al. (2018) is outlined alongside their errors.

Figure 4. A plot showing the Lyα luminosity density fitted with a power law (see equation 2.4). Any data taken from Sobral et al. (2018) is outlined alongside their errors.

equation 14).

$$EW_0(z) = (6.7^{+10}_{-10})z + (80^{+40.}_{-40}) \tag{13}$$

$$f_{\text{esc,LyC}}(z) = (0.0006^{+0.0001}_{-0.0001})EW_0(z) + (0.009^{+0.004}_{-0.004}) \tag{14}$$

It it is worth noting that equation 14 uses observation data from LAEs with a luminosity high enough that they can be detected, leading to a bias in the expressions. As seen in Santos et al. (2020), fainter and lower-mass LAEs have a higher EW_0 and therefore, a higher f_{esc}. This means that equation 14 provides the lower limit to the LyC escape fraction for LAEs.

In addition to an expression relating the fraction of LyC photons from LAEs with EW, a function relating Lyα luminosity density with redshift is required. Table C3 in Sobral et al. (2018) contains Lyα luminosity density values for several different redshift bins ($2.2 \leq z \leq 5.8$). Using these data points an equation relating the Lyα luminosity density to redshift was derived.

Initially, a quadratic fit to this data was taken, which provided figure 3. Whilst this figure provides a good peak for the Lyα luminosity density, the values drop off very quickly either side ($z \approx 4$) and we not expect such a sharp decline in the Lyα luminosity density after $z \approx 4$.

To address the steep drop at $z \lesssim 4$ a Lyα luminosity density fit with a power law was taken (see figure 4). The main complication with fitting the data to a power law is that the luminosity density continually grows as redshift increases. In reality however, the Lyα luminosity density is expected to increase from high redshifts, reach a peak, and then slowly decrease. Furthermore, in both figures 3 and 4 there is also a large amount of uncertainty at higher redshifts. This is due to the extrapolation of the very limited data we took occurring at redshifts during the epoch of reionisation, as well as the formation of the first LAEs.

To reduce this uncertainty, the UV luminosity density was reintroduced once the fit had passed beyond the limit of the Lyα luminosity density. This was done by scaling the UV
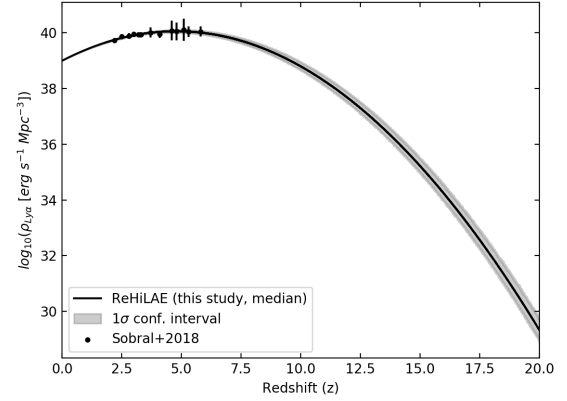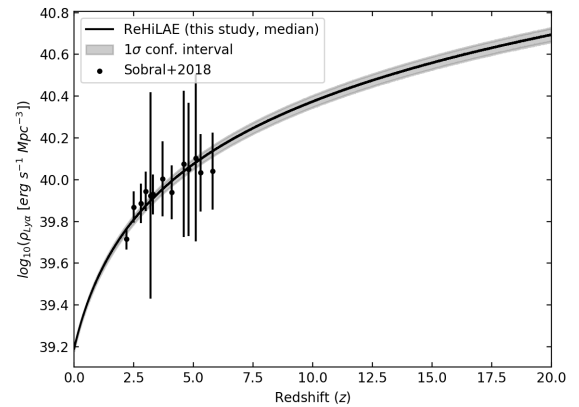
density to so that the cubic UV density fit met the power law fit, leading to the following equations for $\log_{10}(\rho_{Ly\alpha})$:

$$1.2^{+0.18}_{-0.18}\log_{10}(1+z) + 1.2^{+0.025}_{-0.025} \tag{15}$$

and

$$0.001^{+0.001}_{-0.001}z^3 - 0.056^{+0.025}_{-0.025}z^2 + 0.29^{+0.21}_{-0.21}z + 40^{+0.54}_{-0.54} \tag{16}$$

For $z < 5.8$ and $z > 5.8$, respectively. As with equation 14, using a scaled equation ρ_{UV} function in equation 2.4 provides a lower limit of Lyα luminosity density at high redshifts, given only the higher luminosity LAEs appear in observational data, and deriving this from ρ_{UV} runs the risk of excluding higher energy LyC photons that do not fall into this wavelength band.

The equations outlined above are plotted in section 3.4.
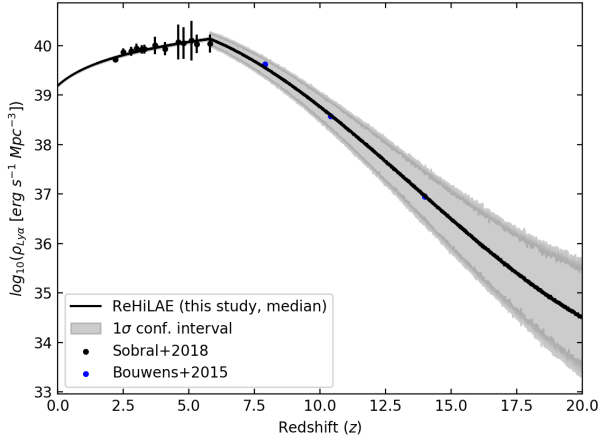
Figure 5. This plot shows the Lyα luminosity density function using the power law fit given by equation 2.4 in addition to the UV cubic fit given by equation 9. We have used the $\rho_{Ly\alpha}$ data from Sobral et al. (2018) and Bouwens et al. (2015) for the ρ_{UV} data which we have then scaled. As seen on the plot, the UV luminosity density was reintroduced once the fit had passed beyond the limit of the Lyα luminosity density.

3 RESULTS

3.1 Markov Chain Monte Carlo

Code was written to utilise the Markov Chain Monte Carlo method and randomise coefficients in the equations $f_{esc,Lyc}$ (14), and $\rho_{Ly\alpha}$ (outlined in section 2.4), and ρ_{UV} (outlined in section 2.2) within their defined uncertainties. Recalling section 2.4, one of our fits for $\rho_{Ly\alpha}$ moves to ρ_{UV} once it passes beyond the limit of the Lyα luminosity density. This is taken into account when altering the coefficients. Each iteration of this code produces new plots of these equations, each with a singly varied coefficient. Repeating this upwards of 1,000 times provides many different possible plots, wherein the median can then be taken. This was done to give an idea of the spread of data for both the ingredients inputted into $Q_{H_{II}}$, and $Q_{H_{II}}$ itself. The probability of picking a particular coefficient was determined using a Gaussian distribution with probability density:

$$p(x) = \frac{1}{\sqrt{2\pi\sigma^2}} exp\left(-\frac{(x-\mu)^2}{2\sigma^2}\right) \qquad (17)$$

where μ is the mean, σ is the standard deviation (inputted as $\frac{1}{5}$ of uncertainties outlined in section 2.4), and x is the range of data used. (See the appendix for graphs mapping out the results of all the iterations). Taking the median of these results and shading between the 16th and 84th percentiles of the median presents both the expected results, and a shaded range of 1σ.

3.2 The UV Framework

Figure 3.2 shows the the dependence of $f_{esc,UV}$ on redshift,
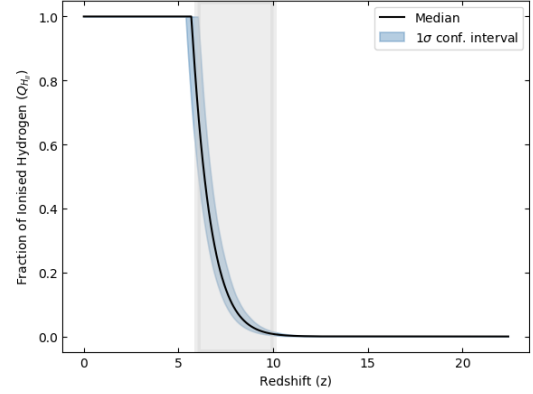
Figure 6. The median and 1σ confidence interval for 10,000 iterations (see section 3.1) of $Q_{H_{II}}$ against redshift using the UV framework and the Robertson model.
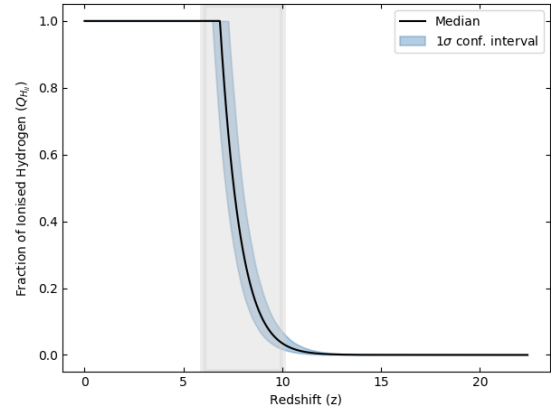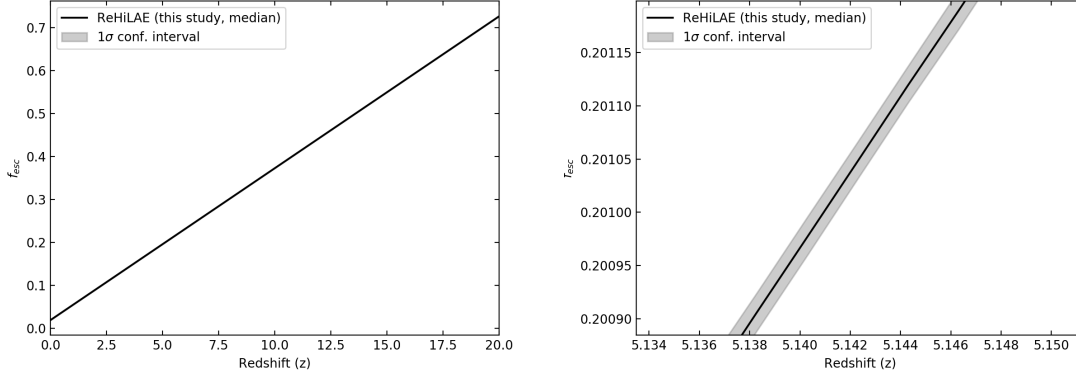

Figure 7. The median and 1σ confidence interval for 10,000 iterations (see section 3.1) of $Q_{H_{II}}$ against redshift using the UV framework and the Faisst model.

as given in equation 7. We find that for redshift $z \geq 5$, $f_{esc,UV}$ exceeds the 0.23 minimum given by Masami Ouchi (2009), representing the minimum value required for any significant contribution to re-ionisation by galaxies with typical stellar populations. Figure 1 shows the change in ρ_{UV} as a function of redshift, as a cubic fit of data from Bouwens et al. (2015). We use this to allow for the variation of ρ_{UV} as an improvement to Robertson's model. We also utilise equation 8 in a similar fashion, to allow the validity of our approximation: $log(\xi_{ion}/Hzerg^{-1}) = 25.4$.

3.3 Final UV Framework Results

3.3.1 Model recreation

From figure 6 we can see the process of re-ionisation as produced by Robertson's model outlined in section 2.1. The process finishes at $z \approx 5.5$, later than the $z = 6$ given by Zaroubi (2012). The recreation of Faisst's model can be seen in figure 7. The added error, implemented as described in section 3.1, is also present on this plot. From these figures we concluded that our recreation of both models was successful, and were a suitable basis for our Lyα framework as outlined in section 2.3.

Figure 8. Variation of f_{esc} against redshift using equation 7. The second graph is simply a zoomed in view of the first as to further emphasise the 1σ confidence interval.
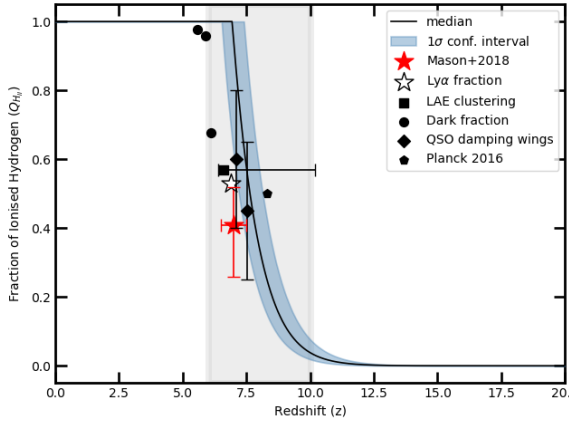
Figure 9. Graph showing the median of 10,000 iterations (see section 3.1) of $Q_{H_{II}}$ (see equation 1) against redshift using the UV model (constant ξ_{ion}) (Sources: see Appendix A)
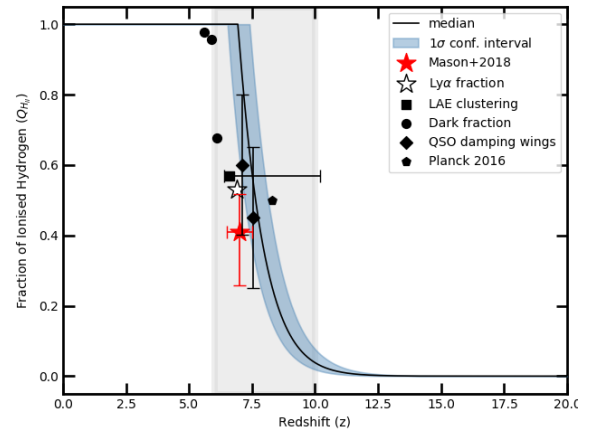
Figure 10. Graph showing the median of 10,000 iterations (see section 3.1) of $Q_{H_{II}}$ (see equation 1) against redshift using the UV model (variable $\xi_{ion}(z)$ using 8) (Sources: see Appendix A)

3.3.2 Changing the UV Model

Figures 9, shows results for our final UV model, assuming a constant ξ_{ion}. We observe that re-ionisation starts at $z \approx 12$ and ends at $z \approx 7$, earlier than the period given in Zaroubi (2012). Figure 10 demonstrates the same model, but utilising equation 8 for ξ_{ion}. This demonstrates minimal change from the $log\left(\xi_{ion}/Hz\ erg^{-1}\right) = 25.4$, and thus justifies the approximation. Figure 11 shows the effect of a variation of C between $C = 1$ and $C = 10$. This results in the end of re-ionisation shifting by $\Delta z \approx 0.3$.

3.4 The Lyα Framework

In section 2.4, the expressions used were outlined for equation 12. For $f_{esc,LYC}$ in $Q_{ion,Ly\alpha}$ (see equation 14 and 11 respectively), values of equivalent width defined by equation 13 were introduced. The plot for our equivalent width expression can be seen in figure 12. Following this, 1,000 iterations were taken using the method outlined in section 3.1 for $f_{esc,LyC}$ with the equivalent width values mapped out above. The resultant plot can be seen in figure 13. To produce results for $\rho_{Ly\alpha}$, many methods were discussed. Sec-

tion 2.4 discusses utilising a quadratic, a power law, and a last fit which uses the power law fit, but returns to the UV model once it passes beyond the limit of the Lyα luminosity density.

3.5 Lyα Framework Results

Our final plot, simulating the re-ionisation of the Universe using the hybrid Lyα luminosity density function (equation 2.4) is shown by figure 17. We have also compared this the re-ionisation curves with the hybrid Lyα luminosity density (figure B2) with the re-ionisation curve curve generated from using (figure 3) in figure 18. It can be seen that using a quadratic fit to our Lyα luminosity density results in the Universe being ionised slightly more quickly than it was when we fit the it with the hybrid function. This supports 2.4 in that the hybrid function provides a lower limit to the Lyα luminosity density. Figure 18 shows the 1σ confidence intervals and it can be seen that the quadratic fit ionises the Universe more quickly than the hybrid function. This is caused by the much steeper gradient for the Lyα luminos-
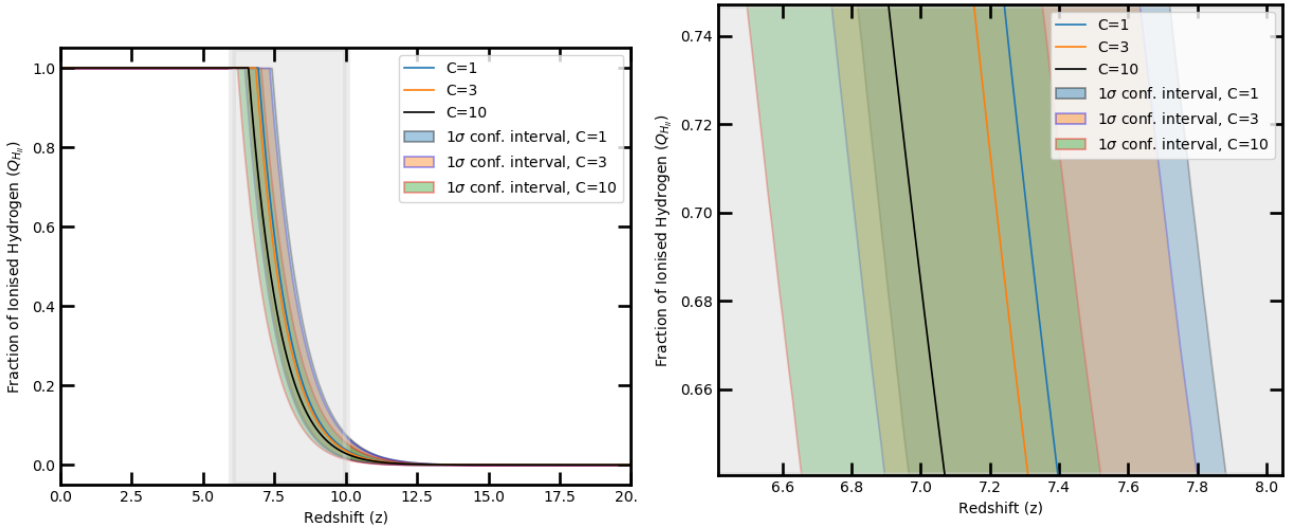
Figure 11. Variation in re-ionisation with clumping factor. The median and 1σ confidence intervals for 10,000 iterations (see section 3.1) of $Q_{H_{II}}$ (see equation 1) against redshift using the UV model for clumping factors of 1, 3, and 10 are shown. The second graph is simply a zoomed in view of the first as to further empathise the data spread.
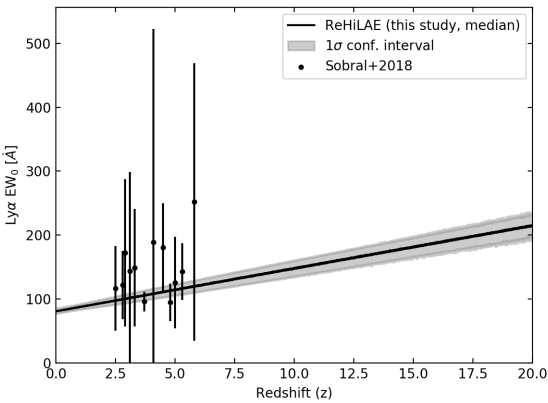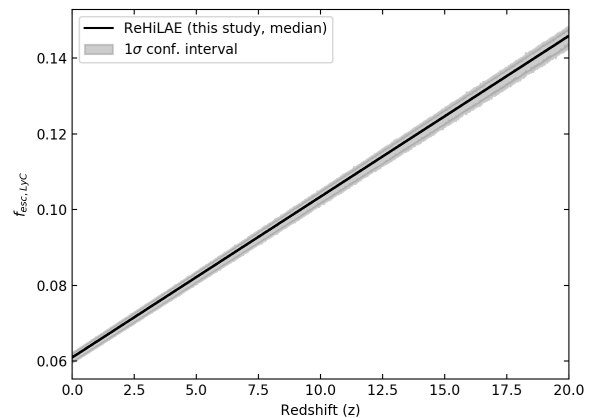

Figure 12. The median and 1σ spread of 1,000 iterations (see section 3.1) of Equivalent Width (see equation 13) against redshift. Data points taken from Sobral et al. (2018) are marked on the graph.

Figure 13. The median and 1σ spread of 1,000 iterations (see section 3.1) of $f_{esc,LyC}$ (see equation 14) against redshift.

ity density at higher redshifts when using the quadratic fit, resulting in higher luminosity densities at higher redshifts.

3.6 Discussion and Comparison

From comparing figures 10 and 17, we can see that with the Lyα method, the median and one sigma range are both comfortably within the range $6 \leq z \leq 10$ which has been highlighted in grey. As discussed in section 1, this is currently the accepted time span for the epoch of re-ionisation. Our UV framework does finish at the agreed upon time but it does also start slightly earlier ($z \approx 12$), whereas our Lyα framework starts later than the UV model ($z \approx 10$) but still finishes just before $z \approx 6$. Not only does this mean that LAEs are capable of re-ionising the Universe but it implies

that they are capable of doing so with a smaller production rate of ionising photons.

It is not surprising that the Lyα framework is producing re-ionisation curves that agree so well with the accepted timeline of the EoR. Given that we have an EW$_0$ varying around 140Å during the EoR which leads to a LyC escape fraction of $\sim$10% (through equation 14). With an escape fraction so much lower than the one stated in Robertson et al. (2013) one might expect our new Lyα model to struggle to re-ionise the Universe by $z = 6$ but due to our new Lyα luminosity density function (2.4) and LAEs being so bright in the Lyα band, we end up with a comparable number of ionising photons in our new framework. If other sources of LyC photons had been included in this study and they were not negligible, then we would expect re-ionisation to finish sooner. However this is not the case (Becker et al. 2001; Barkana 2002), thereby suggesting that other sources of LyC
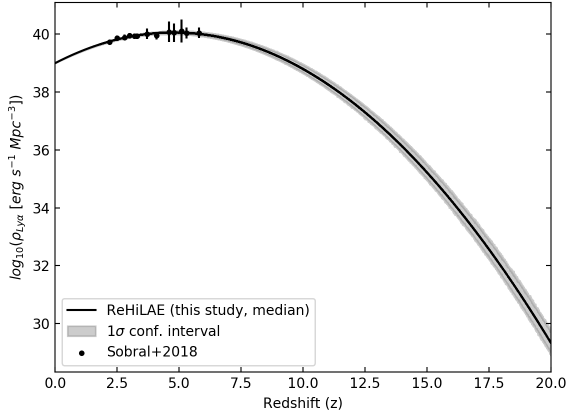
Figure 14. The median and 1σ spread of 1,000 iterations (see section 3.1) of $\rho_{Ly\alpha}$ against redshift using a quadratic fit (see equation 2.4). Data points taken from Sobral et al. (2018) are marked on the graph.
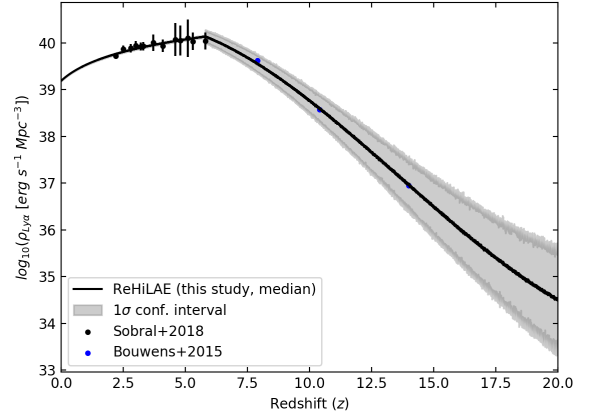
Figure 16. The median and 1σ spread of 1,000 iterations (see section 3.1) of $\rho_{Ly\alpha}$ against redshift using power law fit (see equation 2.4) that moves to the fit defined in equation 9 once it passes beyond the limit of the Lyα luminosity density. Data points taken from Sobral et al. (2018) and Bouwens et al. (2015) are marked on the graph.
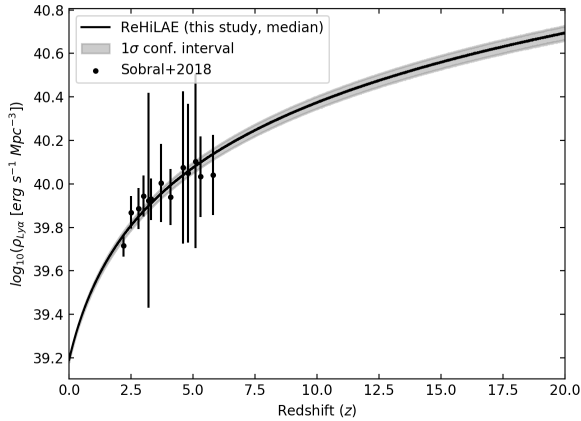
Figure 15. The median and 1σ spread of 1,000 iterations (see section 3.1) of $\rho_{Ly\alpha}$ against redshift using a powerlaw fit (see equation 2.4). Data points taken from Sobral et al. (2018) are marked on the graph.

Figure 17. A graph showing 1000 iterations (see section 3.1) of $Q_{H_{II}}$ against redshift using the Lyα framework (Sources: see Appendix A). Values of $Q_{H_{II}}$ given by various studies are marked on the graph to compare our model against observations.
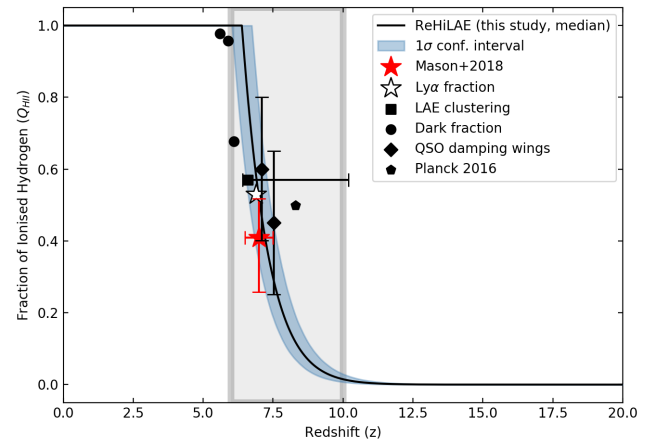
photons are in fact negligible providing further evidence that LAEs are all we need.

4   CONCLUSION

Through the recreation and improvement of UV models of re-ionisation, and then the construction of a model of re-ionisation due to LAEs in our new Lyα, we aimed to discover whether it was possible for the Universe to be re-ionised solely from the contribution of LAEs through solving the differential equation

$$\dot{Q}_{H_{II}} = \frac{\dot{n}_{ion}}{\langle n_H \rangle} - \frac{Q_{H_{II}}}{t_{rec}}$$

Our main results are:

- Our modelling of re-ionisation due to only Lyα demonstrates that re-ionisation occurs within the accepted interval. We can therefore conclude that LAEs are responsible for re-ionisation in our framework.
- Due to the lack of observational data regarding LAEs at high redshifts our newly derived functions for the LyC escape fraction and the Lyα luminosity density (equations 14 and 2.4) provide lower limits to what we expect for these values. In order to have a more realistic model more observed data is needed to allow for a more thorough study. However at the present time only limited data is available to
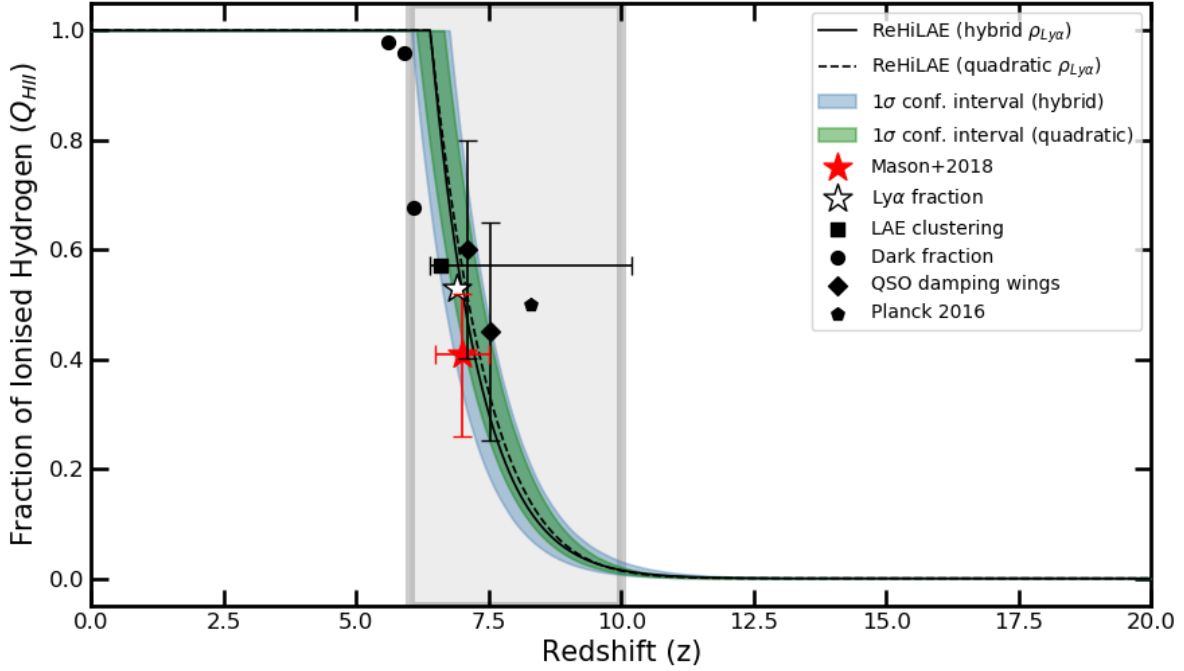
Figure 18. A graph showing 1000 iterations (see section 3.1) of $Q_{H_{II}}$ against redshift using the Lyα framework (Sources: see Appendix A). Values of $Q_{H_{II}}$ given by various studies are marked on the graph to compare our model against observations.

extrapolate data back to large redshift, when observed data can't be gathered.

• Using observational data, we derived simple expressions relating the Lyα EW$_0$ and LyC escape fraction to redshift (equations 13 and 14). For these values, we found that EW$_0 \approx 140$Å and $f_{esc,LyC} \approx 0.1$ for LAEs.

• Despite our hybrid function (2.4) providing a lower limit to the Lyα luminosity density, it is clear from figure 17 that LAEs are more than capable of re-ionising the Universe on their own, even with a smaller production rate of ionising photons than the one used in this model.

Our results show that re-ionisation due ionising photons emitted by LAE can occur within the accepted time frame, within a 1σ error. This model demonstrates an improvement on previous models which focused on the emission of UV photons, starting later and finishing earlier, whilst providing leeway for lower LyC luminosity density.

REFERENCES

Astropy Collaboration et al., 2013, A&A, 558, A33
Barkana R., 2002, New Astronomy, 7, 85
Becker R. H., et al., 2001, The Astronomical Journal, 122, 2850–2857
Bolton J. S., Haehnelt M. G., Warren S. J., Hewett P. C., Mortlock D. J., Venemans B. P., McMahon R. G., Simpson C., 2011, Monthly Notices of the Royal Astronomical Society: Letters, 416, L70
Bouwens R. J., et al., 2015, The Astrophysical Journal, 803, 34
Bouwens R. J., Smit R., Labbé I., Franx M., Caruana J., Oesch P., Stefanon M., Rasappu N., 2016, The Astrophysical Journal, 831, 176
Bruzual G., Charlot S., 2003, Monthly Notices of the Royal Astronomical Society, 344, 1000
Chantry P. J., 1971, The Journal of Chemical Physics, 55, 2746
Dunlop J. S., et al., 2013, Monthly Notices of the Royal Astronomical Society, 432, 3520
Faisst A. L., 2016, The Astrophysical Journal, 829, 99
Fontanot F., Cristiani S., Vanzella E., 2012, Monthly Notices of the Royal Astronomical Society, 425, 1413
Gould R. J., Schréder G. P., 1967, Phys. Rev., 155, 1408
Greig B., Mesinger A., 2016, Monthly Notices of the Royal Astronomical Society, 465, 4838
Greig B., Mesinger A., Haiman Z., Simcoe R. A., 2016, Monthly Notices of the Royal Astronomical Society, 466, 4239
Hunter J. D., 2007, Computing In Science & Engineering, 9, 90
Jones E., Oliphant T., Peterson P., et al., 2001, SciPy: Open source scientific tools for Python, http://www.scipy.org/
Khaire V., Srianand R., Choudhury T. R., Gaikwad P., 2016, Monthly Notices of the Royal Astronomical Society, 457, 4051
Kimm T., Cen R., 2014, The Astrophysical Journal, 788, 121

Landau S. J., Harari D. D., Zaldarriaga M., 2001, Phys. Rev. D, 63, 083505

Liddle A. R., 1999, An introduction to modern cosmology. Wiley, Chichester ; New York

Loeb A., Barkana R., 2001, Annual Review of Astronomy and Astrophysics, 39, 19

Malkan M. A., 1983, ApJ, 268, 582

Mallery R. P., et al., 2012, The Astrophysical Journal, 760, 128

Masami Ouchi Bahram Mobasher K. S. H. C. F. S. M. F. Y. O. N. K. T. M. K. N. S. O., 2009, The Astrophysical Journal, 706, 1136–1151

Mason C. A., Trenti M., Treu T., 2015, The Astrophysical Journal, 813, 21

Mason C. A., Treu T., Dijkstra M., Mesinger A., Trenti M., Pentericci L., de Barros S., Vanzella E., 2018, The Astrophysical Journal, 856, 2

Matthee J., Sobral D., Best P., Khostovan A. A., Oteo I., Bouwens R., Röttgering H., 2016, Monthly Notices of the Royal Astronomical Society, 465, 3637–3655

McGreer I. D., Mesinger A., D'Odorico V., 2014, Monthly Notices of the Royal Astronomical Society, 447, 499

Mesinger A., Aykutalp A., Vanzella E., Pentericci L., Ferrara A., Dijkstra M., 2014a, Monthly Notices of the Royal Astronomical Society, 446, 566

Mesinger A., Aykutalp A., Vanzella E., Pentericci L., Ferrara A., Dijkstra M., 2014b, Monthly Notices of the Royal Astronomical Society, 446, 566

Ouchi M., et al., 2008,] 10.1086/527673, 176, 301

Ouchi M., et al., 2010, The Astrophysical Journal, 723, 869

Peebles P. J. E., 1993, Principles of physical cosmology. Princeton university press

Planck Collaboration et al., 2016a, A&A, 594, A13

Planck Collaboration et al., 2016b, A&A, 596, A108

Razoumov A. O., Sommer-Larsen J., 2010, The Astrophysical Journal, 710, 1239–1246

Robertson B. E., et al., 2013, The Astrophysical Journal, 768, 71

Santos S., et al., 2020, Monthly Notices of the Royal Astronomical Society, 493, 141–160

Sobral D., Matthee J., 2019, Astronomy & Astrophysics, 623, A157

Sobral D., Santos S., Matthee J., Paulino-Afonso A., Ribeiro B., Calhau J., Khostovan A. A., 2018, Monthly Notices of the Royal Astronomical Society, 476, 4725–4752

Stanway E. R., Eldridge J., Becker G. D., 2016, Monthly Notices of the Royal Astronomical Society, 456, 485

Taylor M., 2013, Starlink User Note, 253

Thomas R. M., et al., 2009, MNRAS, 393, 32

Vallini L., Dayal P., Ferrara A., 2012, Monthly Notices of the Royal Astronomical Society, 421, 3266

Van Der Walt S., Colbert S. C., Varoquaux G., 2011, preprint, (arXiv:1102.1523)

Vanzella E., et al., 2010, The Astrophysical Journal, 725, 1011

Verhamme A., Orlitová I., Schaerer D., Izotov Y., Worseck G., Thuan T. X., Guseva N., 2016, Astronomy & Astrophysics, 597, A13

Wilkins S. M., Feng Y., Di-Matteo T., Croft R., Stanway E. R., Bouwens R. J., Thomas P., 2016a, Monthly Notices of the Royal Astronomical Society: Letters, 458, L6

Wilkins S. M., Feng Y., Di-Matteo T., Croft R., Stanway E. R., Bouwens R. J., Thomas P., 2016b, Monthly Notices of the Royal Astronomical Society: Letters, 458, L6

Wise J. H., Cen R., 2009, The Astrophysical Journal, 693, 984

Wise J. H., Demchenko V. G., Halicek M. T., Norman M. L., Turk M. J., Abel T., Smith B. D., 2014, Monthly Notices of the Royal Astronomical Society, 442, 2560–2579

Yajima H., Choi J.-H., Nagamine K., 2011, Monthly Notices of the Royal Astronomical Society, 412, 411

Zaroubi S., 2012, Astrophysics and Space Science Library, p.
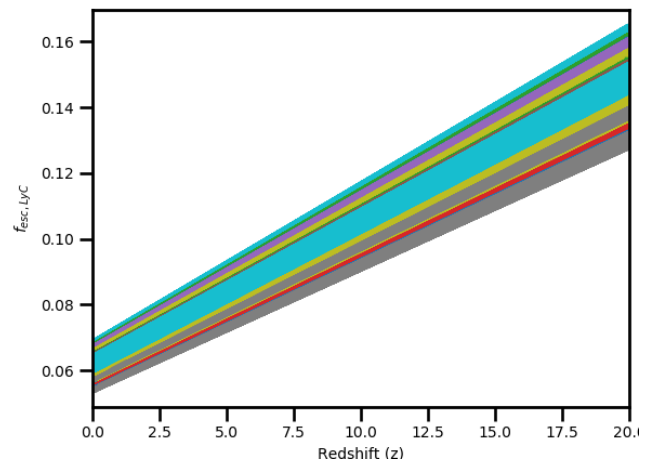
Figure B1. A graph showing 1,000 iterations (see section 3.1) of $F_{esc,Lyc}$ (see equation 14) against redshift.

45–101

Zeldovich Y. B., Kurt V. G., Syunyaev R. A., 1968, Zhurnal Eksperimentalnoi i Teoreticheskoi Fiziki, 55, 278

APPENDIX A: CODE AND DATA AVAILABILITY

All the code and data used to produce the results and graphs throughout this paper is available in a dedicated GitHub repository located at: https://github.com/JP-Carr/ReHILAE

The data from figures 9, 10, 17 and 18 may be found at the following sources:

Mason+2018: (Mason et al. 2018)

Lyα fraction: (Mesinger et al. 2014a)

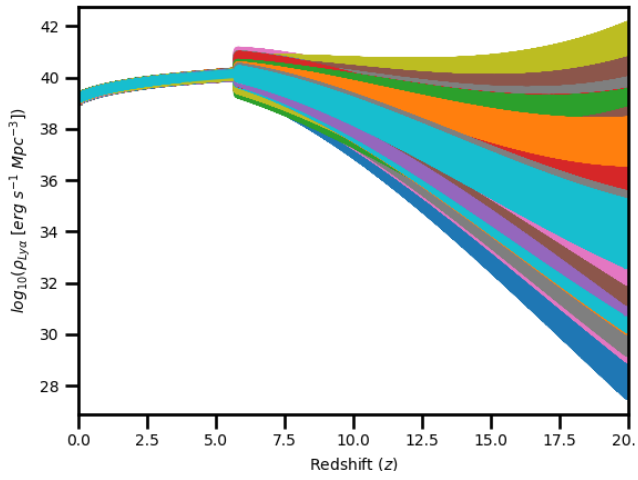LAE clustering: (Ouchi et al. 2010; Mesinger et al. 2014b)

Dark Fraction: (McGreer et al. 2014)

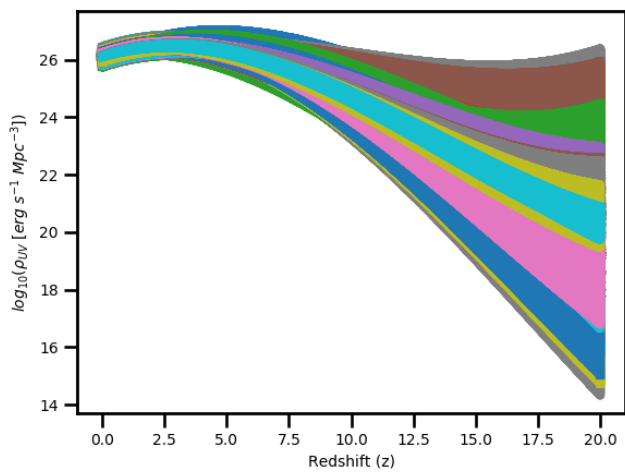QSO damping wings: (Greig & Mesinger 2016; Greig et al. 2016)

Planck 2016: (Planck Collaboration et al. 2016b)

APPENDIX B: ALL ITERATIONS FOR THE UV AND LYα FRAMEWORKS

This paper has been typeset from a T$_E$X/L^{A}T$_E$X file prepared by the author.

Figure B2. A graph showing 1,000 iterations (see section 3.1) of the corrected $\rho_{Ly\alpha}$ (see equation 2.4) against redshift.

Figure B3. A graph showing 1,000 iterations (see section 3.1) of ρ_{UV} (see equation 9) against redshift.